Materials Chemistry and Physics 260 (2021) 124144

Contents lists available at ScienceDirect

Materials Chemistry and Physics

journal homepage: www.elsevier.com/locate/matchemphys

One-step fabrication of Fe_3O_4–Cu nanocomposites: High-efficiency and low-cost catalysts for reduction of 4-nitrophenol

Wenshi Zhao [a,b], Shuo Yang [c], Chenzi Guo [a,b], Jinghai Yang [d,*], Yang Liu [d,**]

[a] Changchun Institute of Optics, Fine Mechanics and Physics, Chinese Academy of Sciences, Changchun, 130033, PR China
[b] University of Chinese Academy of Sciences, Beijing, 100049, PR China
[c] College of Science, Changchun University, Changchun 130022, PR China
[d] Key Laboratory of Functional Materials Physics and Chemistry of the Ministry of Education, Jilin Normal University, Changchun, 130103, PR China

HIGHLIGHTS

- Fe_3O_4–Cu NCs were synthesized by a facile one-pot thermal decomposition method.
- Effect of temperature on structure and catalytic activity of Fe_3O_4–Cu was studied.
- Fe_3O_4–Cu NCs exhibited excellent catalytic activity for reduction of 4-NP.
- Magnetically separable and recyclable Fe_3O_4–Cu NCs showed outstanding stability.

GRAPHICAL ABSTRACT

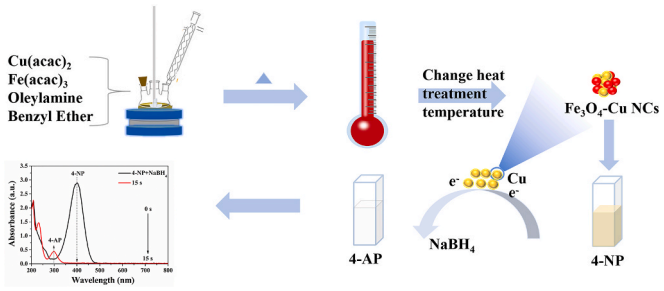

ARTICLE INFO

Keywords:
Fe_3O_4–Cu nanocomposites
Magnetic
Catalytic efficiency
4-Nitrophenol

ABSTRACT

Transition metal Cu nanocrystals have shown promising prospects for degrading organic pollutants. Herein, high-efficiency Fe_3O_4–Cu nanocomposites (NCs) have been successfully synthesized though a facile one-step thermal decomposition method. With a turnover frequency of 6.4 min^{-1}, our Fe_3O_4–Cu NCs (heated temperature: 225 °C) could degrade the 4-nitrophenol in less than 15 s and showed almost unchanged catalytic efficiency (>90%) after recycled reactions up to six times. Furthermore, the influence of the heat treatment on the structure, elemental distribution, magnetic property and catalytic performance of Fe_3O_4–Cu NCs was investigated. As the temperature increased from 225 °C to 285 °C, the saturation magnetization of Fe_3O_4–Cu NCs decreased from 7.27 to 26.2 emu/g, owing to the enlarged mass ratio of Fe_3O_4 nanocrystals: Cu nanocrystals. This work provides the practical design guidance to the large-scale fabrication of high-efficiency and low-cost Fe_3O_4–Cu NCs catalysts, which shows promising future for degrading the nitro compounds in wastewater.

1. Introduction

In the past decades, multifunctional nanomaterials brought tremendous revolution to many fields [1–5]. Compared with noble metal nanocrystals (e.g., Au, Ag and Pt), transition metals, such as Cu nanocrystals, advantage in abundant resources, low cost and high

* Corresponding author.
** Corresponding author.
E-mail addresses: jhyang1@jlnu.edu.cn (J. Yang), liuyang@jlnu.edu.cn (Y. Liu).

https://doi.org/10.1016/j.matchemphys.2020.124144
Received 20 July 2020; Received in revised form 4 November 2020; Accepted 5 December 2020
Available online 8 December 2020

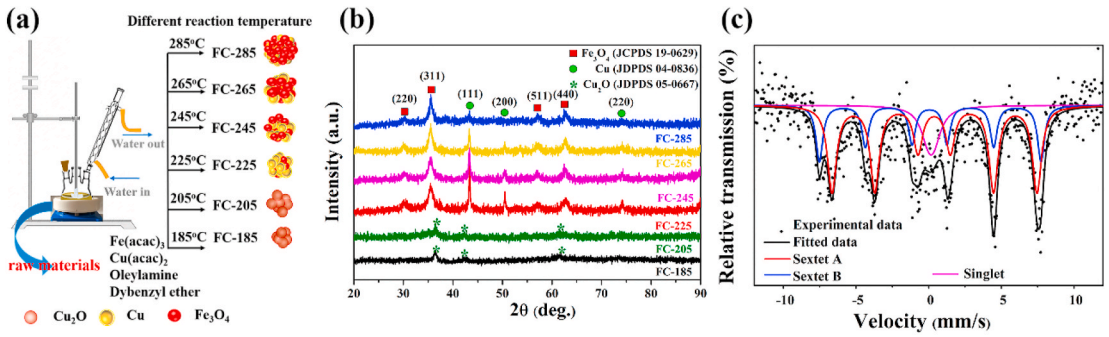

Fig. 1. Schematic diagram of the preparation process of Fe_3O_4–Cu NCs with different reaction temperature (a), XRD patterns of the as-prepared samples heated at different temperatures (185, 205, 225, 245, 265 and 285 °C) (b) and the Mössbauer spectra of FC-285 (c).

stability [6]. Therefore, Cu nanocrystals have become the most promising catalysts for decomposition of environmental pollutants. But similar to noble metal nanocrystals, Cu nanocrystals with high surface energy are inclined to aggregation, which gives rise to a decline in their catalytic efficiency. Though many efforts have been spent in doping semiconductors with transition metals to verify their physical and chemical properties [7–9], the preparation process turns out to be complicated, time-consuming and unsuitable for industrial production. Recent studies indicated that immobilizing Cu nanocrystals onto supporting nanomaterials to achieve multifunctional nanomaterials might be a desirable solution [10]. For example, several reviews reported that carbon-based materials such as carbon nanotubes (CNTs) could be used to support catalysts for catalytic applications [11,12]. But unfortunately, such supporting materials based catalysts usually require multiple washing procedures and thus result in high costs. Owing to the rapid magnetic response, inherent insolubility in most reaction solvents and high compatibility with various materials [13], superparamagnetic Fe_3O_4 nanocrystals are considered as the most ideal magnetic carriers and have attracted lots of attention [14]. Though diverse researches have been accomplished to improve the catalytic activity of Fe_3O_4–Cu nanocomposites (NCs), few efforts were spent in simplifying their fabrication. Preparing and fabricating efficient Fe_3O_4–Cu NCs still includes complex steps, which hinders their practical use. Though Wang et al. achieved a one-step solvothermal method, their Fe_3O_4–Cu NCs could only degrade 4-NP with a turnover frequency (TOF) of ~1 min^{-1}, and the relationship between the Fe_3O_4–Cu NCs and their fabrication temperature remained uninvestigated [15].

Herein, highly efficient Fe_3O_4–Cu NCs were synthesized for the first time via a facile one-step thermal decomposition method. The as-prepared Fe_3O_4–Cu NCs can degrade the 4-nitrophenol (4-NP) within 15 s, and the TOF can reach as high as 6.4 min^{-1}. The catalytic performance of Fe_3O_4–Cu NCs remains almost unchanged after recycled reaction up to six times. The effects of heat treatment temperature on the structural and magnetic properties of Fe_3O_4–Cu NCs were studied. Our study provides the design guidance to the large-scale fabrication of Fe_3O_4–Cu NCs, and paves the way for mass production of high-efficiency, low-cost catalyst.

2. Experimental section

The schematic diagram of the one-step synthesis method is presented in Fig. 1a. The materials, the detailed experimental process and the characterization method can be found in the Supplemental file. Here, Fe $(acac)_3$ and $Cu(acac)_2$ (ac = acetylacetonate) were employed as iron and copper sources, respectively. Oleylamine served as the reducing agent, surfactant and solvent, and benzyl ether was used as the solvent. The samples heated at 185, 205, 225, 245, 265 and 285 °C were prepared and were labeled as FC-185, FC-205, FC-225, FC-245, FC-265 and FC-285, respectively.

3. Results and discussions

The structural characteristics of the samples was studied by X-ray diffractometer (XRD) [16,17], as shown in Fig. 1b. When the heated temperature is below 225 °C, the diffraction patterns of FC-185 and FC-205 peaks at 36.4, 42.3 and 61.3°, which attributed to the (111), (200) and (220) crystal planes of Cu_2O (JCPDS 05–0667), respectively. When the heated temperature increases to 225 °C, the diffraction peaks of Cu_2O disappear and the new diffraction peaks appear at 43.3, 50.4 and 74.1° which correspond to the (111), (200) and (220) crystal planes

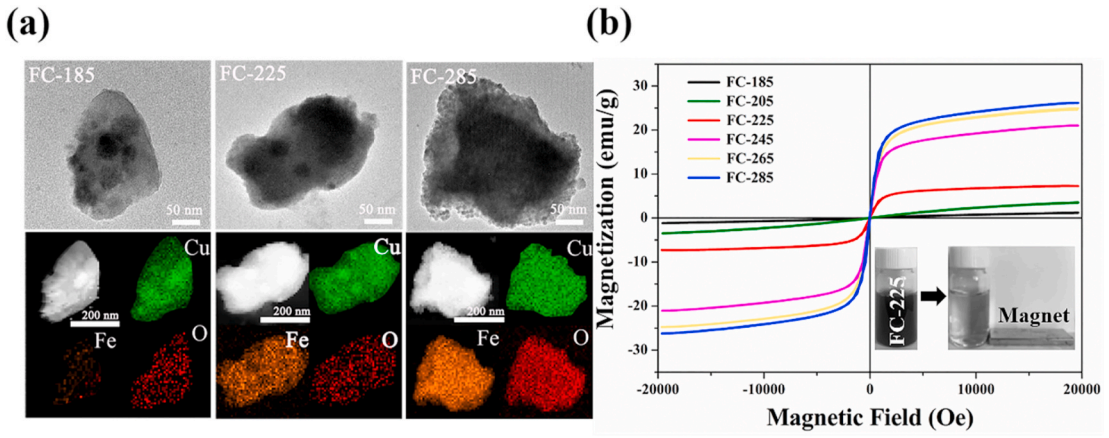

Fig. 2. TEM, STEM and the corresponding EDS elemental mapping images (Cu, Fe and O) of FC-185, FC-225 and FC-285 (a) and magnetic hysteresis (*M-H*) loops of the samples heated at different temperatures of 185, 205, 225, 245, 265 and 285 °C (b). Inset of (b) showed the FC-225 dispersed in deionized water before and after separation by the magnet.

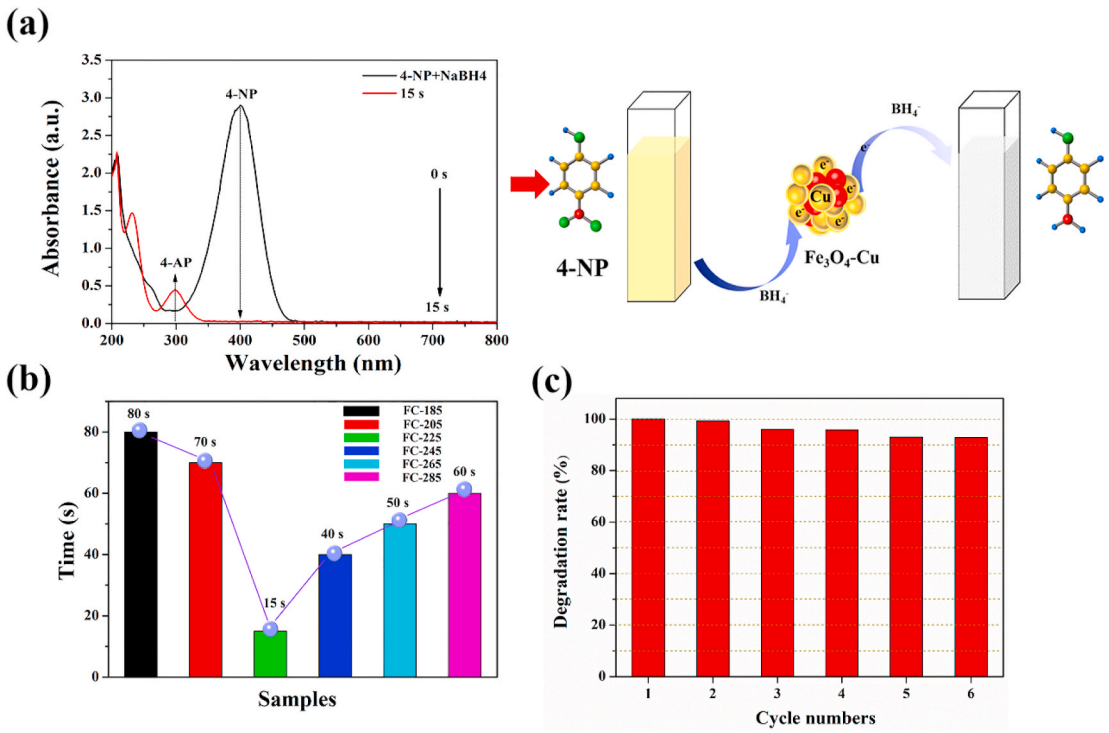

Fig. 3. Time-dependent UV–Vis absorption spectra of 4-NP when catalyzed by FC-225 (a), reaction time of 4-NP reduction with catalysts of FC-185, FC-205, FC-225, FC-245, FC-265 and FC-285 (b) and the recyclability of FC-225 for degrading 4-NP (c).

of Cu (JCPDS 04–0836). Meanwhile, four additional diffraction peaks appear at 30.095, 35.422, 56.942 and 62.515°, which can be well indexed to the (220), (311), (511) and (440) crystal structure of Fe_3O_4 (JCPDS 19–0629) and indicates the start of Fe $(acac)_3$ decomposition. However, in our experiment, $Cu(acac)_2$ is decomposed prior to Fe $(acac)_3$, which is contradictory to the known fact that the decomposition temperature of $Cu(acac)_2$ (286 °C) is higher than Fe $(acac)_3$ (184 °C). A possible explanation is that ligand exchange reaction and subsequent decomposition play a more dominant role than thermal decomposition [18]. Since magnetite Fe_3O_4 and maghemite γ-Fe_2O_3 have similar crystal structures, it is hard to distinguish them by XRD results [19–22]. To solve this issue, we further bring in the Mössbauer spectrum to verify the phase structure of Fe_3O_4 and the corresponding Mössbauer parameters are presented in Table S1. As shown in Fig. 1c, two fitted sextets with double six peak structures are the typical characteristics of magnetite Fe_3O_4. A sites are attributed to the Fe^{3+} ions at tetrahedral interstitial sites, while B sites correspond to the Fe^{2+} and Fe^{3+} ions at octahedral interstitial sites [23]. It can also be observed that the peak intensity ratio of Fe_3O_4 to Cu increases with increasing of heating temperature. Since the intensity of the diffraction peak is positively related to the mass fraction, we can conclude that the content of Fe_3O_4 increases with the heated temperature.

The properties of nanomaterials are closely related to their morphology and detailed structure [24, 25]. Here, the morphology and elemental distribution of FC-185, FC-225 and FC-285 were investigated by transmission electron microscope (TEM), high-angle annular dark-field (HAADF) STEM and the corresponding EDS elemental mapping images, as shown in Fig. 2a. For FC-185, it can be found that the Cu and O atoms are spreaded on the surfaces of Fe_3O_4–Cu NCs, confirming the thermal decomposition of Cu $(acac)_2$. In comparison, few Fe atoms are observed due to the little reduction of Fe $(acac)_3$. When the heated temperature increases to 225 °C, Fe $(acac)_3$ starts to decompose. And the amount of Fe atoms on the surfaces of Fe_3O_4–Cu gradually increases with the heated temperature, which agree with the above XRD results. The vibrating sample magnetometer (VSM) was used to investigate the magnetic properties of the as-obtained samples [26,27]. Magnetic hysteresis (*M-H*) loops of Fe_3O_4–Cu NCs at room temperature are presented in Fig. 2b. Both FC-185 and FC-205 are paramagnetic because the heated temperature is not high enough to affect the decomposition of Fe $(acac)_3$. However, FC-225, FC-245, FC-265 and FC-285 show clear hysteresis loops owing to the formation of superparamagnetic Fe_3O_4 nanocrystals. With the increase of heated temperature, the saturation magnetization significantly increases due to the enlarged mass ratio of Fe_3O_4 to Cu nanocrystals. From the inset of Fig. 2b, although saturation magnetization of FC-225 (7.27 emu/g) is smaller than that of FC-285 (26.2 emu/g), the FC-225 still shows a quick magnetic response to the magnet.

Table 1
Comparison between the performance of FC-225 and some other catalysts when degrading 4-NP.

Catalyst	TOF[a] (min^{-1})	Ref.
FC-225	6.400	this work
$Cu_{0.3}Fe_{0.7}O_x$	2.820	[29]
Pd-rGO-CNT	1.710	[30]
Fe_3O_4–Au MNCs	2.874	[31]
Pt@Ag NPs	0.088	[32]

[a] Turnover frequency (TOF) = (mol of the reacted organic substrate/mol of noble metal) × reaction time (min^{-1}).

The catalytic performance of FC-225 including the reaction time, TOF and recyclability was assessed by monitoring the reduction process of 4-NP with the assistance of $NaBH_4$. Fig. 3a showed that the time-dependent UV–Vis absorption spectra have an intensity peak at 400 nm before the catalytic reduction. After 15 s, the original peak of 4-NP disappears and a new peak rises at 300 nm due to the formation of 4-aminopyridine (4-AP). The degradation mechanism is that BH_4^- and 4-NP are absorbed on the surfaces of the Cu nanocrystals, which facilitate the electron transfer from the donor BH_4^- to the acceptor 4-NP [28]. As shown in the Supplementary video, the thorough reduction of 4-NP can be fulfilled in 15 s. Further, to evaluate the catalytic efficiency of FC-225, we investigated its TOF value and compared it to the reported

ones. As summarized in Table 1, the TOF value of FC-225 for catalyzing 4-NP is as high as 6.4 min^{-1}, which is the highest record to our best knowledge [29–32]. FC-225 exhibits high catalytic performance because its specific surface area can reach up to 63.42 $m^2 g^{-1}$ (Fig. S1), which provides extensive active sites to absorb reactant molecules. In comparison, we applied FC-185 and FC-205 to thoroughly degrading 4-NP, which took 80 and 70 s, respectively. This can be explained by the positive correlation between Fe_3O_4 nanocrystals and the heated temperature [33]. When further increasing the heated temperature from 225 to 285 °C, the catalytic activity of Fe_3O_4–Cu NCs decreases. It is rational that the mass fraction of Cu nanocrystals in Fe_3O_4–Cu NCs relative decreases based on the XRD and TEM results. To demonstrate the stability and reusability of our Fe_3O_4–Cu NCs, the same reduction cycle was repeated for six times, and the catalytic activity of Fe_3O_4–Cu NCs is almost unchanged (Fig. 3c). Based on the above results, we can conclude that our Fe_3O_4–Cu NCs are stable, highly efficient and cost-effective, which poses great potential in the treatment of organic pollutants.

Supplementary video related to this article can be found at https://doi.org/10.1016/j.matchemphys.2020.124144

4. Conclusion

In summary, a facile one-step thermal decomposition approach was proposed for the synthesis of high-efficiency, recyclable Fe_3O_4–Cu NCs catalysts. The structure, magnetic property and catalytic performance of Fe_3O_4–Cu NCs were affected by the heat treatment. When heated at 225 °C, our Fe_3O_4–Cu NCs can degrade 4-NP within only 15 s and the TOF value reaches up to 6.4 min^{-1}. Moreover, the catalytic efficiency of our Fe_3O_4–Cu NCs can maintain as high as 90% of its initial value even after recycled reactions up to six times. To our best knowledge, this is the highest record in 4-NP degradation and outperforms most of the non-metal and noble metal catalysts. Our work enables a novel one-step fabrication of high-efficiency, low-cost and magnetically recyclable nanocatalysts, and provides the guidance for their practical design.

CRediT authorship contribution statement

Wenshi Zhao: Conceptualization, Formal analysis, Writing - original draft. **Shuo Yang:** Investigation. **Chenzi Guo:** Investigation, Resources. **Jinghai Yang:** Resources, Supervision. **Yang Liu:** Resources, Supervision.

Declaration of competing interest

The authors declare that they have no known competing financial interests or personal relationships that could have appeared to influence the work reported in this paper.

Acknowledgement

This work was sponsored by the National Natural Science Foundation of China (Grant Numbers 21676115, 61675090 and 61705020), Program for the development of Science and Technology of Jilin province (Grant Number 20200301043RQ), Thirteenth Five-Year Program for Science and Technology of Education Department of Jilin Province (Grant Number JJKH20200418KJ) and Tianjin Natural Science Foundation of China (Grant Number 16JCYBJC41400).

Appendix A. Supplementary data

Supplementary data to this article can be found online at https://doi.org/10.1016/j.matchemphys.2020.124144.

References

[1] E. Priyadharshini, S. Suresh, S. Gunasekaran, S. Srinivasan, A. Manikandan, Investigation on electrochemical performance of SnO_2-Carbon nanocomposite as better anode material for lithium ion battery, Physica B 569 (2019) 8–13, https://doi.org/10.1016/j.physb.2019.05.029.
[2] T.A. Saleh, M. Tuzen, A. Sari, Magnetic vermiculite-modified by poly (trimesoyl chloride-melamine) as a sorbent for enhanced removal of bisphenol A, J. Environ. Chem. Eng. 7 (2019) 103436, https://doi.org/10.1016/j.jece.2019.103436.
[3] E. Priyadharshini, S. Suresh, S. Srinivasan, A. Manikandan, Structural, optical, thermal and electrochemical analysis of annealed SnO_2–C nanocomposite, Physica B 566 (2019) 17–22, https://doi.org/10.1016/j.physb.2019.04.036.
[4] E. Priyadharshini, S. Suresh, S. Srinivasan, A. Manikandan, Electrochemical performance of TiO_2–C nanocomposite as an anode material for lithium-ion battery, J. Mater. Sci. Mater. Electron. 31 (2020) 6199–6206, https://doi.org/10.1007/s10854-020-03173-5.
[5] T.A. Saleh, Characterization, determination and elimination technologies for sulfur from petroleum: toward cleaner fuel and a safe environment, Trends Environ. Anal. 25 (2020), e00080, https://doi.org/10.1016/j.teac.2020.e00080.
[6] E. Akbarzadeh, H.Z. Soheili, M.R. Gholami, Novel Cu_2O/Cu-MOF/rGO is reported as highly efficient catalyst for reduction of 4-nitrophenol, Mater. Chem. Phys. 237 (2019) 121846, https://doi.org/10.1016/j.matchemphys.2019.121846.
[7] D.K. Manimegalai, A. Manikandan, S. Moortheswaran, Magneto-Optical and photocatalytic properties of magnetically recyclable $MnxZn_{1-x}S$ (x = 0.0, 0.3, and 0.5) nanocatalysts, J. Supercond. Nov. Magnetism 28 (2015) 2755–2766, https://doi.org/10.1007/s10948-015-3089-3.
[8] H. Javadian, M. Ruiz, T.A. Saleh, A.M. Sastre, Ca-alginate/carboxymethyl chitosan/$Ni_{0.2}Zn_{0.2}Fe_{2.6}O_4$ magnetic bionanocomposite: synthesis, characterization and application for single adsorption of Nd^{+3}, Tb^{+3}, and Dy^{+3} rare earth elements from, J. Mol. Liq. 306 (2020) 112760, https://doi.org/10.1016/j.molliq.2020.112760.
[9] L. Arun, C. Karthikeyan, D. Philip, M. Sasikumar, E. Elanthamilan, J.P. Merlin, C. Unni, Effect of Ni^{2+} doping on chemocatalytic and supercapacitor performance of biosynthesized nanostructured CuO, J. Mater. Sci. Mater. Electron. 29 (2018) 21180–21193, https://doi.org/10.1007/s10854-018-0268-6.
[10] S. Liu, J. Jie, Z. Guo, S. Yue, T. Li, A comprehensive investigation on microstructure and magnetic properties of immiscible Cu-Fe alloys with variation of Fe content, Mater. Chem. Phys. 238 (2019) 121909, https://doi.org/10.1016/j.matchemphys.2019.121909.
[11] T.A. Saleh, A.M. Elsharif, S. Asiric, A.R. Mohammed, H. Dafallad, Synthesis of carbon nanotubes grafted with copolymer of acrylic acid and acrylamide for phenol removal, Environ. Nanotechnol. Monit. Manag. 14 (2020) 100302, https://doi.org/10.1016/j.enmm.2020.100302.
[12] I. Ali, A.A. Al-Arfaj, T.A. Saleh, Carbon nanofiber-doped zeolite as support for molybdenum based catalysts for enhanced hydrodesulfurization of dibenzothiophene, J. Mol. Liq. 304 (2020) 112376, https://doi.org/10.1016/j.molliq.2019.112376.
[13] S. Asiri, M. Sertkol, H. Güngüneş, The temperature effect on magnetic properties of $NiFe_2O_4$ nanoparticles, J. Inorg. Organomet. Polym. 28 (2018) 1587–1597, https://doi.org/10.1007/s10904-018-0813-z.
[14] M. Nadimi, A.Z. Saravani, M.A. Aroon, A.E. Pirbazari, Photodegradation of Methylene Blue by a ternary magnetic TiO_2/Fe_3O_4/Graphene oxide nanocomposite under visible light, Mater. Chem. Phys. 225 (2019) 464–474, https://doi.org/10.1016/j.matchemphys.2018.11.029.
[15] Z.Z. Wang, S.R. Zhai, B. Zhai, Q.D. An, One-step green synthesis of multifunctional Fe_3O_4/Cu nanocomposites toward efficient reduction of organic dyes, Eur. J. Inorg. Chem. 10 (2015) 1692–1699, https://doi.org/10.1002/ejic.201403219.
[16] T.A. Saleh, Isotherm, kinetic, and thermodynamic studies on Hg(II) adsorption from aqueous solution by silica- multiwall carbon nanotubes, Environ. Sci. Pollut. Res. 22 (2015) 16721–16731, https://doi.org/10.1007/s11356-015-4866-z.
[17] T.A. Saleh, The influence of treatment temperature on the acidity of MWCNT oxidized by HNO_3 or a mixture of HNO_3/H_2SO_4, Appl. Surf. Sci. 257 (2011) 7746–7751, https://doi.org/10.1016/j.apsusc.2011.04.020.
[18] A.W. Orbaek, L. Morrow, S.J. Maguire Boyle, A.R. Barron, Reagent control over the composition of mixed metal oxide nanoparticles, J. Exp. Nanosci. 10 (2013) 324–349, https://doi.org/10.1080/17458080.2013.832422.
[19] A. Rufus, N. Sreeju, D. Philip, Size tunable biosynthesis and luminescence quenching of nanostructured hematite (α-Fe_2O_3) for catalytic degradation of organic pollutants, J. Phys. Chem. Solid. 124 (2019) 221–234, https://doi.org/10.1016/j.jpcs.2018.09.026.
[20] A. Rufus, N. Sreeju, V. Vidya, D. Philip, Biosynthesis of hematite (α-Fe_2O_3) nanostructures: size effects on applications in thermal conductivity, catalysis, and antibacterial activity, J. Mol. Liq. 242 (2017) 537–549, https://doi.org/10.1016/j.molliq.2017.07.057.
[21] T.A. Saleh, Nanocomposite of carbon nanotubes/silica nanoparticles and their use for adsorption of Pb(II): from surface properties to sorption mechanism, Desalination Water Treat. 57 (2016) 10730–10744, https://doi.org/10.1080/19443994.2015.1036784.
[22] T.A. Saleh, Mercury sorption by silica/carbon nanotubes and silica/activated carbon: a comparison study, J. Water Supply: Res. Technol. 64 (2015) 892–903, https://doi.org/10.2166/aqua.2015.050.
[23] Y. Liu, Y.Y. Zhang, Q.W. Kou, Y. Chen, D.L. Han, D.D. Wang, Z.Y. Lu, L. Chen, J. H. Yang, S. Xing, Eco-friendly seeded Fe_3O_4-Ag nanocrystals: a new type of highly efficient and low cost catalyst for methylene blue reduction, RSC Adv. 8 (2018) 2209–2218, https://doi.org/10.1039/c7ra11348j.

[24] T.A. Saleh, K.G. Vinod, Characterization of the chemical bonding between Al_2O_3 and nanotube in MWCNT/Al_2O_3 nanocomposite, Curr. Nanosci. 8 (2012) 739–743, https://doi.org/10.2174/157341312802884418.
[25] T.A. Saleh, Simultaneous adsorptive desulfurization of diesel fuel over bimetallic nanoparticles loaded on activated carbon, J. Clean. Prod. 172 (2018) 2123–2132, https://doi.org/10.1016/j.jclepro.2017.11.208.
[26] L. Arun, C. Karthikeyan, D. Philip, C. Unni, Optical, magnetic, electrical, and chemo-catalytic properties of biosynthesized CuO/NiO nanocomposites, J. Phys. Chem. Solid. 136 (2020) 109155, https://doi.org/10.1016/j.jpcs.2019.109155.
[27] M. Mustaqeem, K. Mahmood, T.A. Saleh, A. Rehman, M. Ahmad, Z.A. Gilani, M. Asif, Synthesis of $CuFe_{2-x}Er_xO_4$ nanoparticles and their magnetic, structural and dielectric properties, Physica B 58 8 (2020) 412176, https://doi.org/10.1016/j.physb.2020.412176.
[28] Z.Q. Xu, X.H. He, M.W. Liang, L.J. Sun, D. Li, K.N. Xie, L. Liao, Catalytic reduction of 4-nitrophenol over graphene supported Cu@Ni bimetallic nanowires, Mater. Chem. Phys. 227 (2019) 64–71, https://doi.org/10.1016/j.matchemphys.2019.01.065.
[29] H. Yan, X.T. Qin, Y. Yin, Y.F. Teng, Z. Jin, C.J. Jia, Promoted Cu-Fe_3O_4 catalysts for low-temperature water gas shift reaction: optimization of Cu content, Appl. Catal. B Environ. 226 (2018) 182–193, https://doi.org/10.1016/j.apcatb.2017.12.050.
[30] D.R. Kumar, S. Kesavan, M.L. Baynosa, J.J. Shim, 3,5-Diamino-1,2,4-triazole@ electrochemically reduced graphene oxide film modified electrode for the electrochemical determination of 4-nitrophenol, Electrochim. Acta 246 (2017) 1131–1140, https://doi.org/10.1016/j.electacta.2017.06.116.
[31] Y. Chen, T. Wu, G.L. Xing, Y.C. Kou, B.X. Li, X.Y. Wang, Fundamental formation of three-dimensional Fe_3O_4 microcrystals and practical application in anchoring Au as recoverable catalyst for effective reduction of 4-nitrophenol, Ind. Eng. Chem. Res. 58 (2019) 15151–15161, https://doi.org/10.1021/acs.iecr.9b02777.
[32] Z.S. Lv, X.Y. Zhu, H.B. Meng, J.J. Feng, A.J. Wang, One-pot synthesis of highly branched Pt@Ag core-shell nanoparticles as a recyclable catalyst with dramatically boosting the catalytic performance for 4-nitrophenol reduction, J. Colloid Interface Sci. 538 (2019) 349–356, https://doi.org/10.1016/j.jcis.2018.11.109.
[33] Q. Wang, Y. Wang, Re-examination of CuO reduction steps and understanding of the factors influencing the cyclic voltammetry profile of CuO, J. Electrochem. Soc. 165 (2018) A2439–A2445, https://doi.org/10.1149/2.0161811jes.